

Assessment of meteorological climate models as inputs for coastal studies

Debora Bellafiore · Edoardo Bucchignani ·
Silvio Gualdi · Sandro Carniel ·
Vladimir Djurdjević · Georg Umgiesser

Received: 27 January 2011 / Accepted: 21 November 2011 / Published online: 30 December 2011
© Springer-Verlag 2011

Abstract Modeling studies of future changes in coastal hydrodynamics, in terms of storm surges and wave climate, need appropriate wind and atmospheric forcings, a necessary requirement for the realistic reproduction of the statistics and the resolution of small scale features. This work compares meteorological results from different climate models in the Mediterranean area, with a focus on the Adriatic Sea, in order to assess their

capability to reproduce coastal meteorological features and their possibility to be used as forcings for hydrodynamic simulations. Five meteorological datasets are considered. They are obtained from two regional climate models, implemented with different spatial resolutions and setups and are downscaled from two different global climate models. Wind and atmospheric pressure fields are compared with measurements at four stations along the Italian Adriatic coast. The analysis is carried out both on simulations of the control period 1960–1990 and on the A1B Intergovernmental Panel for Climate Change scenario projections (2070–2100), highlighting the ability of each model in reproducing the statistical coastal meteorological behavior and possible changes. The importance of simulated global- and regional-scale meteorological processes, in terms of correct spatial resolution of the phenomena, is also discussed. Within the Adriatic Sea, the meteorological climate is influenced by the local orography that controls the strengthening of north-eastern katabatic winds like Bora. Results show indeed that the increase in spatial resolution provides a more realistic wind forcing for the hydrodynamic simulations. Moreover, the chosen setup and the global climate models that drive the regional downscalings appear to play an important role in reproducing correct atmospheric pressure fields. The comparison between scenario and control simulations shows a small increase in the mean atmospheric pressure values, while a decrease in mean wind speed and in extreme wind events is observed, particularly for the datasets with higher spatial resolution. Finally, results suggest that an ensemble of downscaled climate models is likely to provide the most suitable climatic forcings (wind and atmospheric pressure fields) for coastal hydrodynamic modeling.

Responsible Editor: Chari Pattiaratchi

This article is part of the Topical Collection on *Physics of Estuaries and Coastal Seas 2010*

D. Bellafiore (✉) · S. Carniel · G. Umgiesser
Institute of Marine Science—National Research Council
(ISMAR-CNR), Arsenal e Tesa 104,
Castello 2737/D, 30122 Venice, Italy
e-mail: debora.bellafiore@ismar.cnr.it

E. Bucchignani
Italian Aerospace Research Centre (CIRA), Capua, Italy

E. Bucchignani · S. Gualdi
Centro Euro-Mediterraneo per i Cambiamenti Climatici
(CMCC), Bologna, Italy

V. Djurdjević
Institute of Meteorology, Faculty of Physics,
University of Belgrade, Belgrade, Serbia

V. Djurdjević
South East European Virtual Climate Change Center
(SEEVCCC), Belgrade, Serbia

G. Umgiesser
Coastal Research and Planning Institute (CORPI),
Klaipeda University, Klaipeda, Lithuania

Keywords Climate change · Regional downscaling · Meteorological forcing · Coastal processes · Adriatic Sea

1 Introduction

Half of the European population lives close to the coast (EU 2006) and is exposed to the natural extreme events that characterize this environment. Coastal floodings and severe erosion events are main threats in these areas. In the North Adriatic Sea, an emblematic example is the Venice Lagoon that experiences almost daily floodings in some periods of the year due to the combined action of tides and storm surges. Coastal defenses and new plans for coastal managements start to become main issues for decision makers. Moreover, the evidences raised from the international studies on climate change (Tsimplis et al. 2008; Somot et al. 2008) stress the increasing risk of floodings along the coastal areas, due to the effect of sea level rise combined with the change of meteorological conditions.

Sea level rise can be considered a global phenomenon, even if its impacts are regionally different, while meteorological variations mainly characterize the local scale. As the storm surge and the wave statistics in the coastal zone are governed by this latter forcing, the assessment of meteorological inputs is needed to correctly reproduce the present climate and to identify the degree of uncertainty for future scenarios.

It has been widely recognized by both the scientific community and the Intergovernmental Panel for Climate Change (IPCC) that modeling is a useful tool for the study of climate change on the global and, recently, on a regional scale (Somot et al. 2008). It allows the investigation of different CO₂ emission scenarios (IPCC 2007). As major forcings driving the global ocean circulation, the first studies on the global climate change dealt with the heat and water air–sea balance, providing estimates of the oceanic and atmospheric heat content and precipitation (Giorgi et al. 2004). Model ensembles defined a commonly accepted set of values in terms of CO₂ emissions, amount of rain and evaporation and, as a consequence, a global range in sea level variation (IPCC 2007). All these aspects, however, are mainly connected with the general thermohaline ocean circulation, as a driver of the global climate.

The same variables were studied in regional-scale applications by Somot et al. (2006), namely for one of the semi-enclosed basins that more strongly affects the general thermohaline circulation, the Mediterranean Sea. Resulting heat and water fluxes and the consequent sea

level variation were the focus of several works (Somot et al. 2008; Tsimplis et al. 2008).

The general interest in downscaling the global climate information on a regional and local scale is due to the increasing need to face the climate change effects in the most vulnerable areas, like the coasts. To our knowledge, this is the first attempt to compare different downscaled regional climate model (RCM) meteorological datasets in the Adriatic Sea. More specifically, wind and atmospheric fields will be analyzed on the local scale, focusing on the coastal zone. The Adriatic Sea can be considered an ideal natural laboratory to study local meteorological effects, due to its characteristics: It is narrow and latitudinally elongated, shallow in the north and deep in the south, and surrounded in the northern part by a large mountain chain that affects the wind climate. Therefore, it experiences highly varying wind regimes, particularly along the coasts, superposed to the synoptic atmospheric pressure changes that affect the sea level. More specifically, the North Adriatic is characterized by two main wind regimes: one, generally cold and dry, of katabatic origin (blowing down slopes due to gravity) coming from northeast (Bora) and one, wetter and warmer, blowing from southeast (Sirocco) (Orlić et al. 1992). Approaching the coastal zone, land–sea interactions, like sea breeze, tend to increase the directional variability of these wind fields.

A first experiment to investigate possible climatic variations on the hydrodynamics in the Adriatic Sea was presented by Bergamasco et al. (2003). In that work, scenarios of possible changes of the heat fluxes, even if not computed by climate models, were used to investigate plausible changes in the three-dimensional general basin circulation. In another work, considering the outputs produced by the global atmospheric model ECHAM4 (ECMWF Hamburg atmospheric general circulation model developed at the Max Planck Institute for Meteorology—Roeckner et al. 1996), Pasarić and Orlić (2004) presented a first assessment of meteorological forcings in the Adriatic Sea, as simulated with a global atmospheric global climate model (GCM). Heat fluxes, water fluxes, and wind fields were analyzed for the control period (1970–1999) and for a future scenario with the doubling of CO₂ concentration in the atmosphere (2060–2089). However, the spatial resolution of 1.125° did not allow any consideration on coastal areas.

In the past, only relatively few studies analyzed meteorological variables produced by downscalings over the Adriatic Sea region from global climate simulations. A further step was done in verifying the meteorological variables already considered on the global scale, i.e., precipitation, air, and sea temperature, on limited

areas. An example is provided by Zampieri et al. (2010) who consider the dynamics of the northern Adriatic area. Vichi et al. (2003) investigated the effects of regional climate change scenarios on the Adriatic Sea ecosystem by means of a one-dimensional model forced by ECHAM4, identifying an increase in the basin mean temperature. However, both these efforts did not consider either the wind fields or the atmospheric pressure.

In this work, we are more interested in the meteorological effects on the coastal regions, which are mainly influenced by the wind and atmospheric pressure fields rather than by the thermohaline variations. To our knowledge, Woith et al. (2006) represents the only attempt to verify the capability to reproduce, in a climate perspective, wind fields and induced storminess in the North Sea coastal zone. A similar approach will be used in this work focusing mainly on the northern part of the Adriatic Sea, although analyses on wind and atmospheric pressure fields on the whole basin will be presented as well.

In order to determine how the global scale meteorological information might affect the coastal zone of the northern Adriatic, we consider climate model downscaled fields. The local effects due to different model implementations, different global model nesting, and different spatial resolution will be analyzed for the present climate and future scenarios.

In Section 2, the meteorological datasets and the measurements used to validate the control period will be presented. A description of each model setup will be

provided. In Section 3, first the mean and extreme values statistics for the control period will be discussed, also analyzing differences due to seasonality. As a second step, the IPCC A1B scenario will be explored, computing the variations from the control period and trying to identify the degree of uncertainty in providing such variation ranges. In Section 4, results are discussed and in Section 5, conclusions and recommendations are drawn.

2 Methods—measured and climate model datasets

Wind and atmospheric pressure datasets resulting from different climate models are analyzed, both for a control period and the IPCC A1B scenario. Additionally, their statistics are compared with measurements for the control period. In this section, the basic information on the measured datasets, the characteristics of models, and their setup are described, and some information on the analyses performed on the datasets are provided.

2.1 Measurements

To evaluate the quality of the climate models in reproducing wind statistics, a comparison with some of the longest measured datasets in the North Adriatic is made. The chosen stations are Trieste, Venice Tesserà, and Ravenna (Fig. 1). Bari, in the South Adriatic, is also

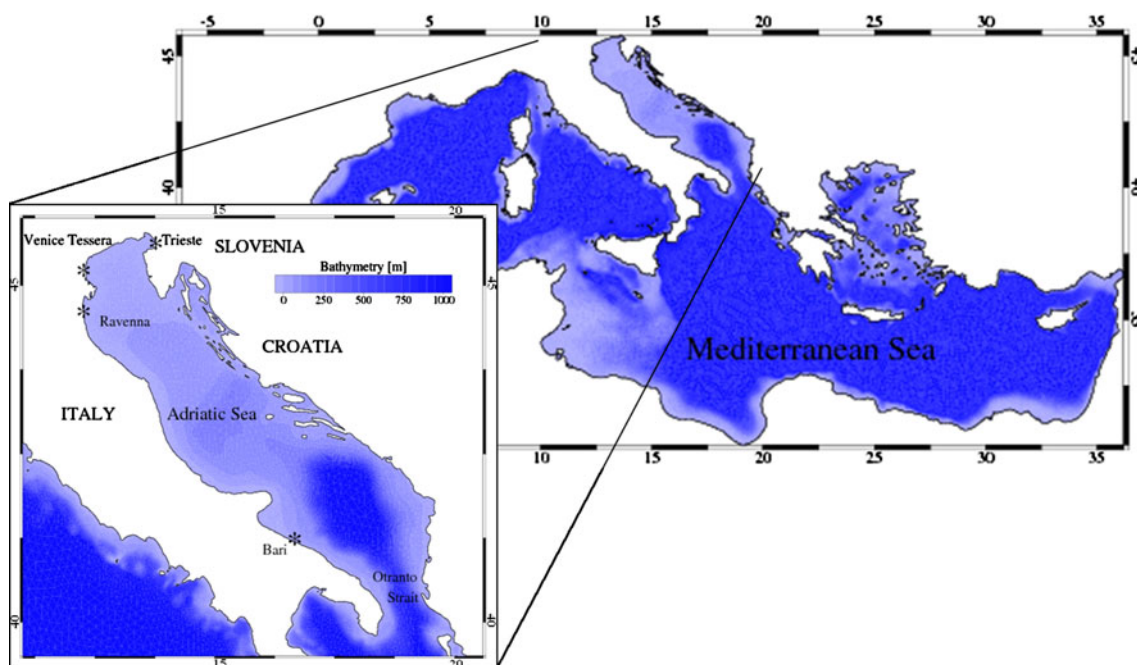


Fig. 1 Study area. Location of wind stations

considered to evaluate model–measurement discrepancies also in a different geographic area. Data are from the SYNOP National Aeronautics dataset that covers the period 1958–2004 (the 1960–1990 period simulated by the models has been taken into account) and are provided every 3 h.

2.2 Model description

The first model described is Eta Belgrade University—Princeton Ocean Model (EBU-POM) that is a coupled atmosphere–ocean regional climate model (Djurdjevic and Rajkovic 2010; Krzic et al. 2011). The atmospheric component is the Eta—National Centers for Environmental Prediction model, a hydrostatic, primitive equation, grid-point model. For the soil and surface processes, the model uses the NOAH land surface model (LSM) model and, for the first model layer, turbulence is parameterized by the Monin–Obukhov approach with the viscous sub-layer implementation. In the rest of the atmosphere, the turbulence scheme is Mellor–Yamada 2.5. The convection parameterization is Bets–Miller–Janic, and for radiation, the Goddard radiation package is used. The model has a quasi-horizontal vertical coordinate with a step-like representation of topography. The ocean component is the POM, a three-dimensional, primitive equation, grid-point model with sigma vertical coordinate (Blumberg and Mellor 1986). The model is free surface, computes the complete thermodynamics, and has a second-order Mellor–Yamada 2.5 turbulence closure scheme. The two models are coupled through the exchange of atmospheric surface fluxes and sea surface temperature (SST) (Djurdjevic and Rajkovic 2008).

CLM (Rockel et al. 2008) is the second model we used. It is the climate version of the Consortium of Small-Scale Modelling (COSMO) model, which is the operational non-hydrostatic mesoscale weather forecast model developed by the German Weather Service. It is non-hydrostatic and can be applied in

cloud resolving scales. The impact of turbulent motions on the non-resolvable scales is taken into account by Reynolds averaging. The parameterization settings include a Tiedtke convection scheme (Tiedtke 1989) with a moisture convergence closure, a turbulence scheme with prognostic turbulent kinetic energy, and a Kessler scheme for grid-scale precipitation (Kessler 1969), which treats cloud ice diagnostically. COSMO-CLM is a finite difference model that runs on a rotated spherical coordinate system. COSMO-CLM offers three options for the vertical coordinate: a reference-pressure based coordinate, a height-based coordinate, and the height-based smooth level vertical coordinate. In this current version, COSMO-CLM is not coupled with an oceanic model, and the boundary conditions on the sea are prescribed SSTs obtained by coupled GCM integrations. The soil is modeled with the soil and vegetation multilevel model TERRA-LM.

Both EBU-POM and COSMO-CLM models can be used with high spatial resolution (of the order of few kilometers). This allows a better description of orography (all relieves present in the area) with respect to the global models, where there is an over-/underestimation of valleys and mountain heights, resulting in errors for the orographic precipitation estimation, closely related to terrain height.

2.3 The model setup

All the models consider limited domains; therefore, their boundary conditions are obtained from global climate models. Results are provided for the control period (1960–1990) and for the A1B IPCC scenario (2070–2100). The main characteristics of the analyzed datasets are summarized in Table 1.

The EBU-POM dataset will be hereafter called E dataset. The atmospheric model domain has spatial resolution of 25 km, 32 vertical levels, and covers most of the Euro-Mediterranean region. POM is set up with a resolution of 0.2° and with 21 vertical

Table 1 Main characteristics of the employed meteorological datasets

| Experiment | RCM | AOGCM | Resolution (km) | Spatial domain | Vertical levels | Time output (h) |
|------------|-----------|-------------------|-----------------|------------------------------|-----------------|-----------------|
| E | EBU-POM | SINTEX-G (ECHAM4) | 25 | 2–20° E 40–52° N | 42 | 6 |
| C14E4 | COSMO-CLM | SINTEX-G (ECHAM4) | 14 | 2–20° E 40–52° N | 40 | 6 |
| C14E5 | COSMO-CLM | CMCC-MED (ECHAM5) | 14 | 2–20° E 40–52° N | 40 | 6 |
| C8E5 | COSMO-CLM | CMCC-MED (ECHAM5) | 8 | 2–20° E 40–52° N | 40 | 6 |
| S18E5 | COSMO-CLM | ECHAM5-MPIOM | 18 | 10.7–36.9° E 34.5–69.9° N | 32 | 3 |

levels, covering the Mediterranean basin. Initial and 6-h lateral boundary conditions are obtained from SINTEX-G atmosphere–ocean global circulation model (Gualdi et al. 2008). Over the Atlantic and the Black Sea, which are treated as uncoupled seas inside the model domain, SST from SINTEX-G is taken as a bottom boundary condition.

The COSMO-CLM model provides four different datasets, three of them produced for this study at the Italian Aerospace Research Centre (CIRA) and the fourth at the Deutscher Wetterdienst (DWD), available for the climate community. The three sets of simulations from CIRA are performed in the domain 2–20° E, 40–52°N, for the time period 1965–2100. Further details on the three simulations are the following:

- C14E4 dataset: spatial resolution 14 km, 40 vertical levels. Boundary conditions from the global model SINTEX-G, whose atmospheric component is ECHAM4 (T106 ~120 km spatial resolution, 12 h time resolution, 360 days yearly)
- C14E5 dataset: spatial resolution 14 km, 40 vertical levels. Boundary conditions from the global model EuroMediterranean Center for Climate Change (CMCC-MED; Scoccimarro et al. 2011), whose atmospheric component is ECHAM5 (T159 ~80 km spatial resolution, 6 h time resolution, 365 days yearly)
- C8E5 dataset: spatial resolution 8 km, 40 vertical levels. Boundary conditions from the global model CMCC-MED, whose atmospheric component is ECHAM5 (T159 ~80 km spatial resolution, 6 h time resolution, 365 days yearly)

The fourth COSMO-CLM set of simulations, provided by the DWD, is hereafter called S18E5 dataset. It is initialized and forced six hourly by global coupled model ECHAM5–Max Planck Institute Ocean Model (MPIOM; Jungclaus et al. 2006) and provides results with a spatial resolution of 18 km. This model implementation introduces a substantial smoothing of the Caucasus Mountains orography to the constant height of 150 m, which is the mean height in the ECHAM5/MPIOM model for that region.

2.4 Dataset analyses description

The model datasets described above are analyzed to assess their capability to reproduce the observed statistics and to evaluate their outputs in a future climate scenario. In order to do this, the modeled meteorological fields are bilinearly interpolated on a finite element grid to extract wind and atmospheric pressure time series in the same position of the meteorological stations (Fig. 1).

A preliminary assessment of the mean and extreme wind speed and atmospheric pressure fields during the control period (1960–1990) is carried out. The analyses on the control period consist of the comparison of mean values with measurements and the evaluation of the modeled wind direction reproduction. Extreme events generally occur with high wind speeds and low atmospheric pressure. Therefore, the 99th percentile wind speed values, the 1st percentile atmospheric pressure values and the anomaly of the latter from the mean are computed and compared with measurements. Moreover, a seasonal analysis of wind regimes is also performed.

As a second step, the climate scenario wind and atmospheric pressure datasets are compared with the control period values (both for means and extreme events) in the four stations described above. Finally, in order to investigate spatial differences in the whole Adriatic Sea, scenario–control period mean difference maps of wind speed and atmospheric pressure are discussed for each dataset. The whole analysis takes into account the effects related to the increase in the spatial resolution of regional climate models and the influence of the boundary conditions imposed from the global models.

3 Results

3.1 Control period

3.1.1 Modeled and measured wind and atmospheric pressure fields comparison

The modeled and measured mean wind speed and atmospheric pressure values were compared for the three selected stations in the North Adriatic (Venice Tesserà, Trieste, and Ravenna) and for Bari, in the south (Fig. 1). The mean wind speed in Venice Tesserà is better reproduced by dataset E than by the others, though underestimated (11%). The high-resolution COSMO-CLM datasets (C14E4, C8E5, S18E5) do not reproduce the wind speed statistics in the northwestern Adriatic area. In these simulations, the wind speed appears to be overestimated by about 40% (Table 2). However, they appear to perform better in the other stations. Considering the two datasets C14E5 and C8E5, both laterally forced by CMCC-MED global climate model but running with different spatial resolutions, surprisingly it appears that the less resolved of the two better matches the mean wind speed (almost perfect matching in Ravenna for C14E5 dataset vs overestimation ~30% for C8E5). The C8E5 dataset generally overestimates

Table 2 Control period (1960–1990): mean values and relative model–measurement differences (in percent) for wind speed (upper panel) and atmospheric pressure (lower panel), for Venice Tessera, Trieste, Ravenna, and Bari stations

| Stations | Data | E | C14E4 | C14E5 | C8E5 | S18E5 |
|---------------------------------------|---------|---------|---------|---------|---------|---------|
| Wind speed–control period (1960–1990) | | | | | | |
| Mean value (m/s) | | | | | | |
| VeT | 3.7 | 3.3 | 5.3 | 5.2 | 5.4 | 5.4 |
| Ts | 3.8 | 1.1 | 3.6 | 4.2 | 4.8 | 4.2 |
| Ra | 3.7 | 0.9 | 3.1 | 3.7 | 4.8 | 3.3 |
| Ba | 3.8 | 1.4 | 4.0 | 4.5 | 4.9 | 4.7 |
| Model–data percentage difference (%) | | | | | | |
| VeT | | –11 | 42 | 40 | 44 | 46 |
| Ts | | –70 | –3 | 13 | 28 | 11 |
| Ra | | –76 | –16 | 0 | 30 | –11 |
| Ba | | –63 | 4 | 18 | 29 | 23 |
| Atmospheric pressure–control period | | | | | | |
| Mean value (hPa) | | | | | | |
| VeT | 1,015.6 | 1,018.6 | 1,016.9 | 1,015.6 | 1,016.0 | 1,015.8 |
| Ts | 1,015.4 | 1,019.2 | 1,018.0 | 1,015.6 | 1,016.9 | 1,015.9 |
| Ra | 1,015.2 | 1,019.2 | 1,018.0 | 1,015.6 | 1,016.9 | 1,015.9 |
| Ba | 1,014.4 | 1,019.2 | 1,018.0 | 1,015.6 | 1,016.8 | 1,015.9 |
| Model–data percentage difference (%) | | | | | | |
| VeT | | 0.3 | 0.1 | 0.0 | 0.0 | 0.0 |
| Ts | | 0.4 | 0.3 | 0.0 | 0.2 | 0.1 |
| Ra | | 0.4 | 0.3 | 0.0 | 0.2 | 0.1 |
| Ba | | 0.5 | 0.4 | 0.1 | 0.2 | 0.2 |

VeT Venice Tessera,
Ts Trieste, Ra Ravenna,
Ba Bari

the mean wind speed value in all the stations ($\sim 29\%$), while the other two COSMO-CLM datasets, with lower resolution (C14E5) and also different setup (S18E5), have a less uniform behavior in different basin areas (Table 2).

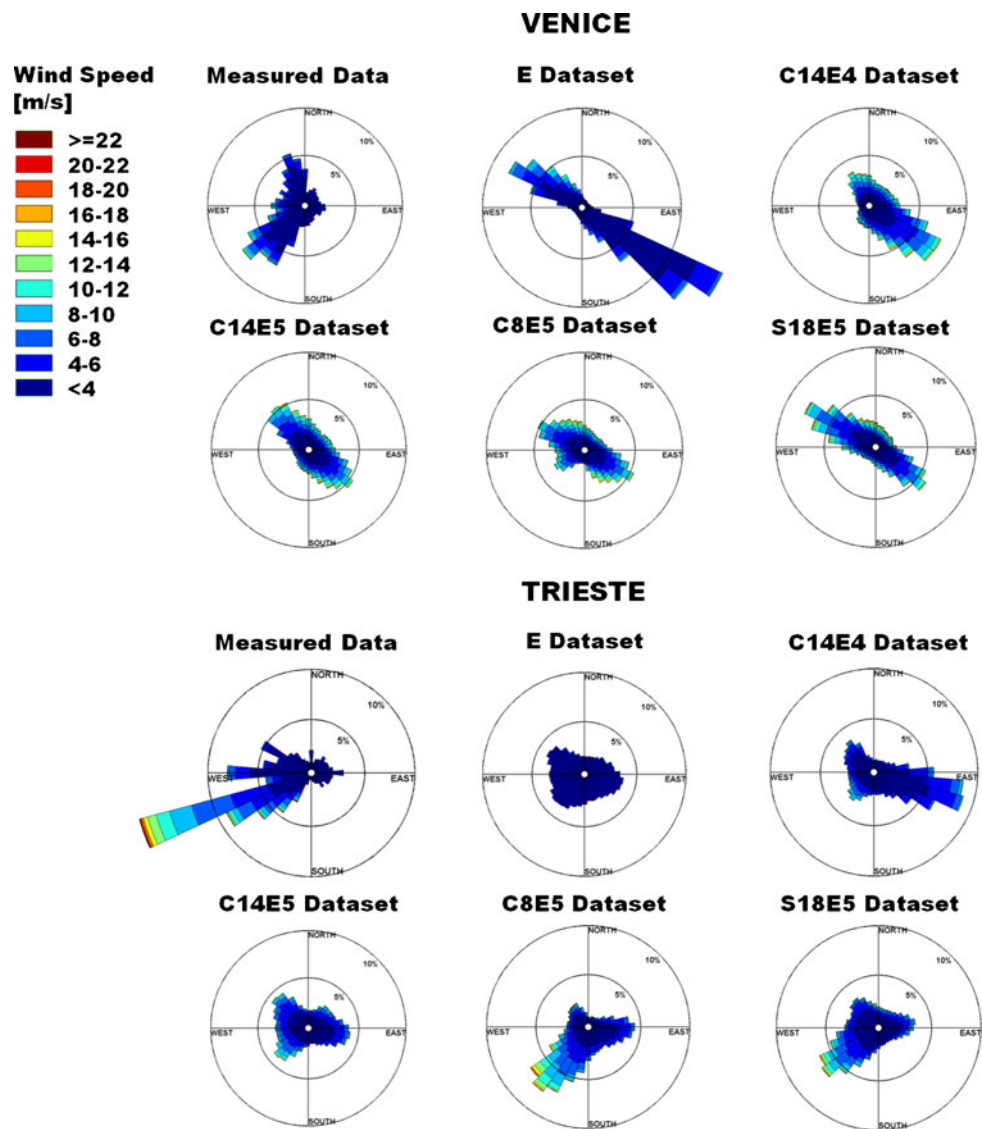
Atmospheric pressure is reproduced better than wind by all models in all stations, showing relative differences lower than 0.4% (E dataset). Almost a perfect match is seen in Venice Tessera station for the C14E5, C8E5, and S18E5 datasets. Wind speed, related to pressure gradients, is in general more difficult to model than pressure itself. The two variables are characterized by different spatial scales: The atmospheric pressure varies significantly within synoptic scales, while the wind field is variable even on the coastal sub-mesoscale. Therefore, different models' resolution and setups are most likely affecting wind than atmospheric pressure field reproduction.

Concerning the capability to reproduce wind fields, a specific comparison is carried out on wind directions. In Fig. 2, wind roses for measured and modeled data in the control period are shown. These graphs provide information on the major wind regimes experienced in each station and their intensity. Measured data clearly show that both in Venice Tessera and Trieste, which are the northernmost stations, Bora winds are dominant reaching speeds up to 18 m/s (Fig. 2). Venice Tessera experiences also a second wind regime, from southeast, Sirocco. However, all model datasets exhibit problems

in reproducing the wind regimes found for Venice Tessera station. The E dataset, in particular, produces fictional wind directions with winds blowing along the southeast axis. The most realistic dataset is C8E5 that reproduces both Bora and Sirocco regimes, even if with a lower percentage compared with observations (Bora modeled $\sim 3\%$ vs measured $\sim 7\%$). The S18E5 simulation shows some skill in reproducing the Sirocco regimes but fails in the Bora ones (Fig. 2). C8E5 and S18E5 are the two datasets that better reproduce the main wind regimes characterizing the northern part of the Adriatic Sea, particularly in Trieste (wind speed reaches ~ 16 m/s, Fig. 2). The other two stations are less characterized by specific wind regimes, also due to the lack of orographic effects. Therefore, Ravenna and Bari observations show a more distributed wind rose and lower wind speeds (Fig. 3). The C14E4 dataset is the one that better reproduces the Ravenna condition, while the better resolved C8E5 simulation, as well as the two other datasets downscaled from ECHAM5, C14E5, and S18E5, do not show a good agreement with station data. Bari wind direction is well modeled by the E dataset, while, in contrast with observations, C14E4 registers strong winds to the east and C8E5 and S18E5 show winds blowing from northeast.

Moreover, the model performance in terms of extreme wind events is evaluated. While the E dataset clearly underestimates the wind speed extremes ($\sim 20\%$ in Venice Tessera and $\sim 68\%$ in the other stations,

Fig. 2 Wind roses showing the main measured and modeled wind regimes for the control period (1960–1990) for Venice Tesserà and Trieste stations. The directions indicate where wind is blowing to



see Table 3), a less homogeneous behavior is seen for the other datasets. C14E4 and C14E5 overestimate the extremes in the northwestern part (Venice Tesserà) and underestimate them in Trieste, Ravenna, and Bari. Interestingly, the dataset with the highest resolution (C8E5) shows a systematic overestimation of the wind extremes (~12%, Table 3), even if this is the dataset in better agreement with observations. The 1st percentile values of atmospheric pressure (Table 4) is slightly underestimated by the models downscaled from ECHAM5 (underestimation 0.3% as an average) while the ones downscaled from ECHAM4 tend to be overestimated (around 3% as an average). These results suggest that for atmospheric pressure extreme event reproduction, the influence of the boundary conditions of the RCMs is important. Moreover, the computation of the 1st percentile anomaly from the mean shows how

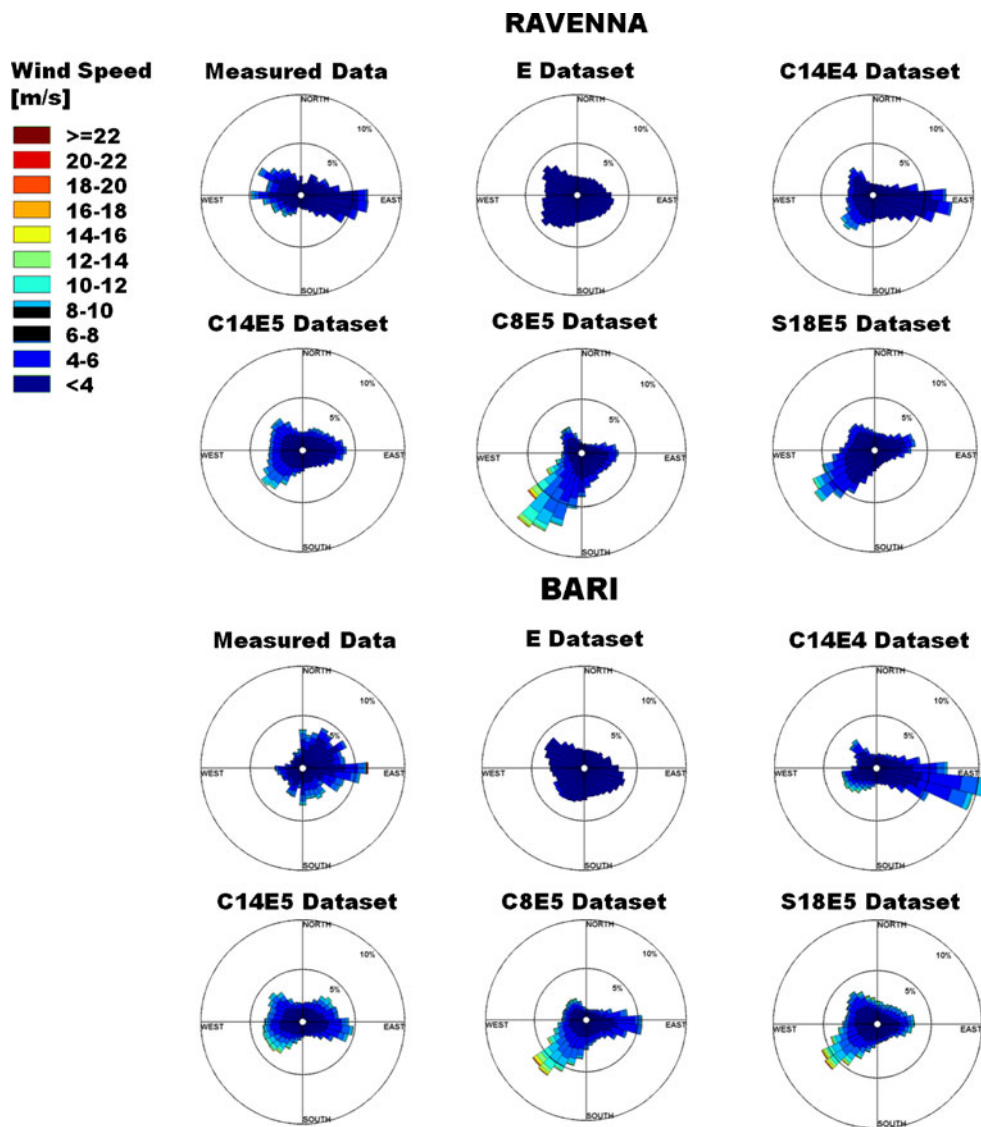
pressure variations are in the order of 20 hPa, both for models and measurements. Therefore, according to the inverted barometer effect (Pugh 2004), a sea level rise in the order of 20 cm should be expected due to these low atmospheric pressure extremes. All model datasets appear to be able to reproduce this tendency.

3.1.2 Seasonal analysis of wind regimes

In order to shed some light on these preliminary considerations, we investigated the seasonal character of modeled wind speed means and extremes (99th percentile) and their deviation from measured data. The intent is to verify how the models behave in seasons mainly governed by specific wind regimes.

In Venice Tesserà, wind speed means are not matched by the models (Table 5), except for the E

Fig. 3 Wind roses showing the main measured and modeled wind regimes for the control period (1960–1990) for Ravenna and Bari stations. The directions indicate where wind is blowing to



dataset that, however, is not able to capture seasonal changes in wind direction regimes (seasonal wind roses not shown here). Models downscaled from ECHAM5 generally reproduce better the mean wind speeds

in Venice during summer (overestimation ~20%, Table 5). The highest resolved dataset (C8E5) reproduces the observed seasonal regimes both in Venice and Trieste, matching the strong Bora winds

Table 3 Extreme event statistics for the control period (1960–1990): 99th percentile values for wind speed (upper panel) and relative model–measurement differences (lower panel) [%] for Venice Tesserà, Trieste, Ravenna, and Bari stations

| Stations | Data | E | C14E4 | C14E5 | C8E5 | S18E5 |
|---|------|------|-------|-------|------|-------|
| Wind speed–control period (1960–1990) | | | | | | |
| 99th percentile value (m/s) | | | | | | |
| VeT | 12.9 | 10.3 | 14.3 | 14.3 | 15.0 | 15.7 |
| Ts | 13.2 | 4.1 | 10.3 | 11.7 | 14.4 | 13.1 |
| Ra | 12.9 | 3.3 | 8.8 | 10.4 | 14.2 | 10.1 |
| Ba | 12.9 | 5.0 | 11.3 | 12.6 | 14.4 | 14.6 |
| Model–data 99th percentile difference (%) | | | | | | |
| VeT | | –20 | 11 | 11 | 16 | 22 |
| Ts | | –69 | –22 | –11 | 9 | –1 |
| Ra | | –74 | –32 | –19 | 11 | –22 |
| Ba | | –61 | –12 | –2 | 12 | 13 |

VeT Venice Tesserà,
Ts Trieste, *Ra* Ravenna,
Ba Bari

Table 4 Extreme event statistics for the control period (1960–1990): 1st percentile atmospheric pressure values (upper panel), relative model–measurement differences (in percent) (central panel) and anomaly from mean value (lower panel) for Venice Tesserà, Trieste, Ravenna, and Bari stations

| Stations | Data | E | C14E4 | C14E5 | C8E5 | S18E5 |
|---|-------|---------|-------|-------|-------|-------|
| Atmospheric pressure–control period (1960–1990) | | | | | | |
| 1st percentile (hPa) | | | | | | |
| VeT | 995.3 | 1,002.4 | 999.9 | 995.1 | 995.2 | 994.7 |
| Ts | 995.5 | 1,000.2 | 998.3 | 992.0 | 993.6 | 991.2 |
| Ra | 995.3 | 1,000.2 | 998.3 | 992.0 | 993.5 | 991.2 |
| Ba | 996.8 | 1,000.2 | 998.4 | 992.1 | 993.5 | 991.2 |
| Model–data 1st percentile difference (%) | | | | | | |
| VeT | | 0.71 | 0.46 | −0.02 | −0.01 | −0.06 |
| Ts | | 0.47 | 0.28 | −0.35 | −0.19 | −0.43 |
| Ra | | 0.49 | 0.3 | −0.33 | −0.18 | −0.41 |
| Ba | | 0.34 | 0.16 | −0.47 | −0.33 | −0.56 |
| 1st percentile anomaly from mean value (hPa) | | | | | | |
| VeT | −20.3 | −16.2 | −17.0 | −20.5 | −20.8 | −21.1 |
| Ts | −19.9 | −19.0 | −19.7 | −23.6 | −23.3 | −24.7 |
| Ra | −19.9 | −19.0 | −19.7 | −23.6 | −23.4 | −24.7 |
| Ba | −17.6 | −19.0 | −19.6 | −23.5 | −23.3 | −24.7 |

VeT Venice Tesserà,
Ts Trieste, Ra Ravenna,
Ba Bari

in autumn and winter and the Sirocco winds in summer. The latter regime is also found by S18E5. Extreme wind values in Trieste are reproduced by C8E5 with a 99th percentile overestimation lower than ~10% in autumn and summer and an underestimation of about ~10% in winter and spring. C14E4 is the dataset that shows the best agreement with data in the central and southernmost stations: In Ravenna, the winter wind direction regime is found in both C14E4 and C14E5. The latter is able to reproduce the extreme wind values in Ravenna (underestimation of ~7% in summer and autumn and of ~17% in winter and spring—

Table 5). It also reproduces the mean and extreme wind speed in Bari during winter and spring (99th percentile ~7% and ~−3%, Table 5). On the other hand, in these two stations, all models, except the E dataset, reproduce clearly directionally distinguishable wind regimes while measurements show a high directional variability.

The evaluation of model performances in each station shows the ability of the models in reproducing the measured wind fields under certain conditions, but it is not possible to identify one dataset as the most accurate over the whole domain.

Table 5 Mean and 99th percentile wind speed model–measurement differences (in percent) for the control period (1960–1990), seasonally analyzed for Venice Tesserà, Trieste, Ravenna, and Bari stations

| Stations | Seasonal wind speed model–data difference (%) | | | | | | | | | |
|----------|---|-------|-------|------|-------|-----------------------|-------|-------|------|-------|
| | Mean value | | | | | 99th percentile value | | | | |
| | E | C14E4 | C14E5 | C8E5 | S18E5 | E | C14E4 | C14E5 | C8E5 | S18E5 |
| Winter | | | | | | | | | | |
| VeT | −7 | 49 | 87 | 94 | 93 | −25 | 7 | 16 | 20 | 28 |
| Ts | −71 | −12 | 0 | 22 | 5 | −70 | −38 | −31 | −13 | −22 |
| Ra | −73 | −6 | 5 | 47 | −4 | −73 | −29 | −16 | 20 | −19 |
| Ba | −68 | −11 | 7 | 22 | 17 | 346 | −8 | 7 | 26 | 28 |
| Spring | | | | | | | | | | |
| VeT | −26 | 14 | 42 | 45 | 47 | −36 | −9 | 7 | 10 | 13 |
| Ts | −73 | −14 | 7 | 19 | 12 | −78 | −40 | −26 | −10 | −14 |
| Ra | −77 | −15 | 4 | 27 | −4 | −78 | −35 | −19 | 7 | −19 |
| Ba | −71 | −21 | −2 | 6 | 0 | −68 | −19 | −3 | 10 | 13 |
| Summer | | | | | | | | | | |
| VeT | −2 | 58 | 21 | 18 | 19 | −1 | 38 | 8 | 17 | 15 |
| Ts | −66 | 9 | 29 | 34 | 16 | −63 | −8 | −6 | 7 | −9 |
| Ra | −73 | −7 | 18 | 41 | 2 | −66 | −14 | −7 | 17 | −15 |
| Ba | −63 | 5 | 16 | 16 | 8 | −47 | 15 | 17 | 25 | 17 |
| Autumn | | | | | | | | | | |
| VeT | 21 | 97 | 54 | 64 | 68 | −8 | 24 | 14 | 21 | 29 |
| Ts | −67 | 5 | 13 | 34 | 9 | −70 | −24 | −13 | 5 | −3 |
| Ra | −71 | −5 | 9 | 50 | −5 | −71 | −21 | −7 | 28 | −10 |
| Ba | −58 | 18 | 22 | 35 | 23 | −51 | 13 | 23 | 41 | 42 |

VeT Venice Tesserà,
Ts Trieste, Ra Ravenna,
Ba Bari

3.2 A1B scenario–control period comparison

Analyzing the mean wind speed variations between the future A1B IPCC scenario and the control period, it is evident that the majority of the models simulates a general decrease in the four coastal stations, higher for models downscaled from ECHAM4 (E and C14E4 dataset, average about $\sim -6\%$ and $\sim -6.4\%$, Table 6). The only exception is represented by C14E5 that shows a smaller decrease in Trieste, Ravenna, and Bari. Considering the mean atmospheric pressure, all stations either show no variations or small increase. The largest increase is $\sim +0.2\%$ for the S18E5 dataset (Table 6).

The largest decrease in the wind extreme values is depicted by the E and C14E4 datasets ($\sim -9\%$ and $\sim -6\%$, Table 6), while the other datasets register smaller decreases. However, all stations identify the same tendency. Additionally, the 1st percentile atmospheric pressure anomaly from the mean value shows a slight increase in the low atmospheric pressure values, confirmed by nearly all models. Therefore, extreme low pressure values detected in the control period are not reached in the simulation under A1B scenario. To support this evidence, the Kolmogorov–Smirnov hypothesis test was applied for each station on the control period and A1B scenario wind and atmospheric pressure time series. The computed p values are almost 0 everywhere, confirming that differences in mean and distribution between them are significant.

A more comprehensive picture of the mean wind speed and atmospheric pressure scenario–control period changes can be provided for the whole Adriatic

Sea. Figures 4 and 5 show the absolute variation between the averaged wind speed (atmospheric pressure) over the periods 2070–2100 (A1B scenario) and 1960–1990 (control period). Figure 4 clarifies that a decrease tendency for mean wind speed is evident in the whole basin. Generally, higher decreases are registered in the open sea than along the coasts and are at most around -0.5 m/s. Spatial responses are different for each model, and we are interested on verifying how the models behave moving offshore from the coastal zones (studied in the four stations). The lowest wind speed variation is provided by the E dataset (range $[-0.2, 0]$ m/s), with a uniform response of the coastal areas, on both sides of the basin. No significant changes are seen between areas that experience the presence of orography behind their coasts (i.e., Trieste) and flat areas (Ravenna). A similar response can also be seen in S18E5, even if with stronger changes. C14E4 shows an interesting situation on the whole eastern coast, with the highest decrease in wind speed (-0.4 m/s). The basin response seems to be longitudinally dependent, more than latitudinally, showing, in any case, a non-significant decreases along the Italian coast. The same tendency, but even less pronounced, is seen for C14E5. As expected, the two datasets C14E5 and C8E5, which differ only in spatial resolution, show similar maps. The more resolved model reproduces higher wind speed decreases also in the western coast of the Adriatic Sea and in the northern end of the basin.

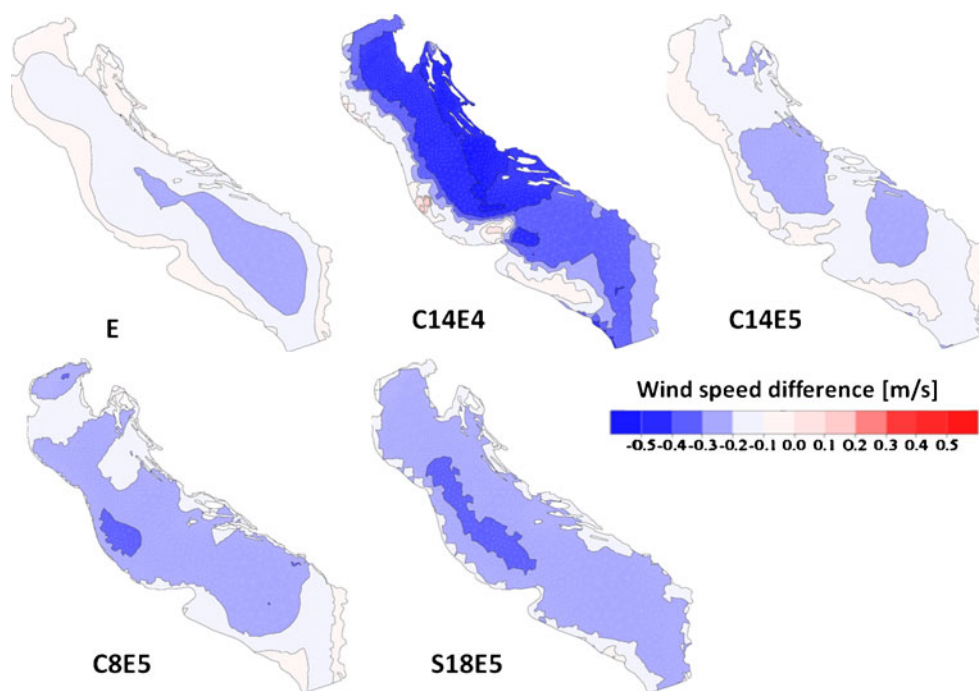
The mean atmospheric pressure differences shown in Fig. 5 present a more uniform behavior of each modeled dataset. All models define indeed a general

Table 6 A1B scenario–control period relative differences (as a percentage, $100 \frac{A1B-CP}{CP}$), for mean atmospheric pressure and wind speed values (upper panel) and for extreme events values (1st percentile atmospheric pressure anomaly from mean value and wind speed 99th percentile—lower panel), for Venice Tesserà, Trieste, Ravenna, and Bari stations

VeT Venice Tesserà,
Ts Trieste, *Ra* Ravenna,
Ba Bari

| Stations | E | C14E4 | C14E5 | C8E5 | S18E5 |
|--|------|-------|-------|------|-------|
| Mean atmospheric pressure difference (%) | | | | | |
| VeT | 0.0 | 0.0 | 0.1 | 0.1 | 0.2 |
| Ts | 0.0 | 0.0 | 0.1 | 0.1 | 0.2 |
| Ra | 0.0 | 0.0 | 0.1 | 0.1 | 0.2 |
| Ba | 0.0 | 0.0 | 0.1 | 0.1 | 0.2 |
| Mean wind speed difference (%) | | | | | |
| VeT | -7.9 | -6.3 | -4.3 | -5.3 | -4.7 |
| Ts | -5.3 | -6.7 | -0.5 | -4.5 | -4.6 |
| Ra | -5.5 | -5.0 | -0.4 | -4.0 | -3.2 |
| Ba | -5.2 | -7.7 | -0.9 | -4.2 | -5.1 |
| 1st percentile atmospheric pressure anomaly difference (%) | | | | | |
| VeT | -4.6 | -5.3 | -4.8 | -4.8 | -3.5 |
| Ts | -5.1 | -1.7 | -0.1 | 1.4 | -1.3 |
| Ra | -5.1 | -1.6 | 0.3 | 1.4 | -1.6 |
| Ba | -5.2 | -1.8 | 0.0 | 1.2 | -1.3 |
| 99th percentile wind speed difference (%) | | | | | |
| VeT | -5.0 | -3.9 | -4.4 | -4.6 | -0.1 |
| Ts | -9.3 | -6.1 | -2.7 | -3.7 | -2.2 |
| Ra | -9.7 | -4.9 | -1.8 | -4.0 | -3.4 |
| Ba | -9.7 | -6.1 | -2.6 | -1.7 | -1.6 |

Fig. 4 Average wind speed difference between the A1B scenario and the control period for the E, C14E4, C14E5, C8E5, and S18E5 datasets

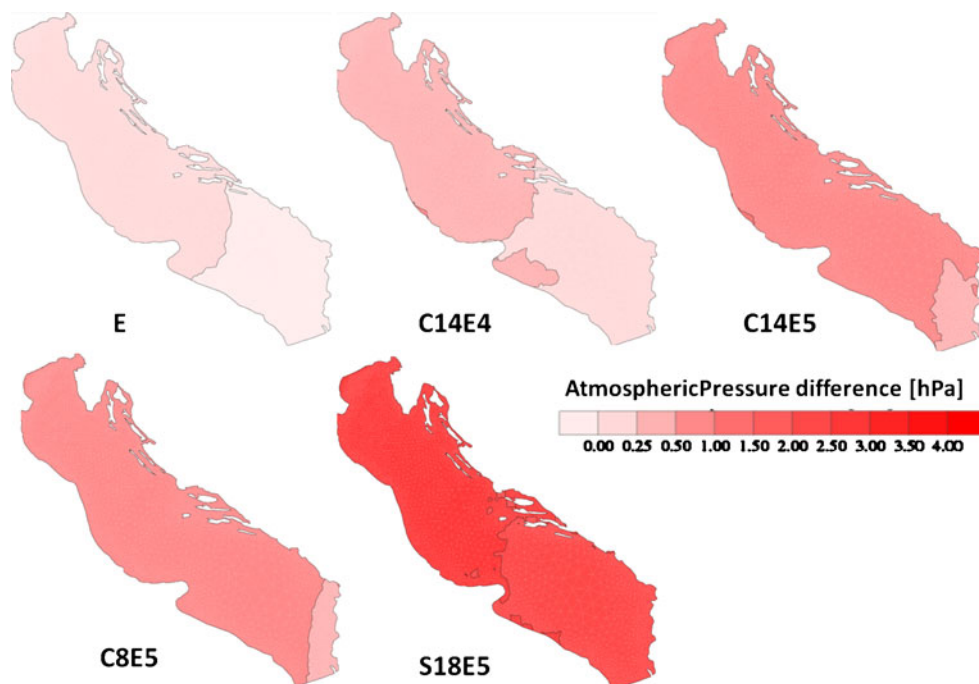


increase in the mean atmospheric pressure, higher in the north, lower in the south. In any case, the variations are bracketed in the range [0, 4] hPa that corresponds to water level displacements due to atmospheric pressure in the order of few centimeters (Pugh 2004). As in the case of wind speed, the E dataset shows the smallest A1B scenario–control period variations, actually close to 0, while the largest excursion is provided by the S18E5 dataset.

4 Discussion

The results of the previous section lead to a first assessment on the performances, in a climatic perspective, of GCM downscalings to RCMs, what concerns wind and atmospheric pressure fields. These are the main forcings for coastal hydrodynamics, and their behavior is deeply linked with the spatial scale of analysis: The atmospheric pressure is more linked with large-

Fig. 5 Average atmospheric pressure difference between the A1B scenario and the control period for the E, C14E4, C14E5, C8E5, and S18E5 datasets



scale processes and characterized by relatively homogeneous variations on larger geographical areas, while the wind speeds (and directions) are more affected by local processes. It is therefore possible that, as an example, the highest resolved dataset (C8E5) can better reproduce winds without showing significant improvements in the atmospheric pressure modeling at the same time. Atmospheric pressure reproduction may be more influenced by models' setup and boundary conditions. When comparing the measured and modeled datasets, a number of aspects have to be stressed. Venice Tesserà, differently from the other stations, is not exactly located along the coast but more toward the Venice Lagoon, i.e., in a border region close to models land–sea mask. Since the measured time series for the control period is compared with the closest coastal point, this can justify less satisfactory results. Pirazzoli and Tomasin (2003) explain how the wind speeds, moving from the coastal areas to the inner part of the Venice Lagoon, experience an attenuation, also due to urbanization. Therefore, it is likely that in Venice Tesserà station, weaker wind speeds are measured. Table 2 shows that mean wind speed values in Venice Tesserà are generally overestimated ($\sim +40\%$), except for the E dataset (that simulates small wind speeds on the whole basin and therefore obtains more similar values in this station).

Considering all the stations, C14E5 (14 km) performs better than C8E5 (8 km) in wind reproduction, suggesting that a simple increase of the resolution does not automatically improve the results, at least in terms of mean wind field (see also Signell et al. (2005)). Resolution, in any case, plays an important role in defining the correct wind regimes. From the wind rose shown in Fig. 2, it is evident that, particularly in Trieste, the wind directions are better matched by C8E5 than C14E5. On the other hand, resolution is not the only difference between the datasets, since different setups are used for the COSMO-CLM simulations performed at the CIRA Institute (C14E4, C14E5, C8E5) and for the one provided by the World Data Center for Climate (S18E5). The latter considers a smoothing of the Balkan orography, to avoid some numerical errors even if modeling a less realistic mountain configuration. In Trieste, which is the station that mostly experiences the effects of the katabatic Bora winds, this assumption provides better results both in the extreme events modeling ($\sim -1\%$ vs higher underestimation from the other models, Table 3) and in the direction reproduction (Fig. 2).

Atmospheric pressure fields are reproduced better than wind by all models in all stations, being mainly driven by the larger spatial scale. The models' performances in reproducing this variable does not seem to

be dependent on resolution. The less resolved of the COSMO-CLM datasets downscaled from ECHAM5 (i.e., C14E5 and S18E5) seem to better convey the information from the global climate model to the regional downscaling (Tables 2 and 3).

Moreover, boundary conditions resulting from different global climate models, with different parameterizations and setups, can affect the meteorological field reproduction. This could explain some mismatches, for example that the mean atmospheric pressure differences of E and C14E4 datasets are higher than those of the other datasets (Table 2).

The seasonal analysis shows that the E dataset does not identify the main wind regimes in the different seasons, forecasting a rather fixed direction on the axis southeast in Venice Tesserà and presenting a spread wind rose for the other stations. This could be connected with the spatial resolution, which is the lowest in the considered datasets. This does not permit the accurate orography modeling needed for wind regimes identification, particularly in the northern part of the basin. The most resolved dataset (C8E5) differentiates the seasonal wind regimes but does not match the measured mean wind speed (see Table 5). Better results are obtained by this dataset when reproducing extreme wind events, once again showing how a higher resolution can help in modeling intense directional fixed wind regimes (Table 5). Examples are given by Bora winds in Trieste in winter and autumn and Sirocco winds in Venice Tesserà and in Bari in spring and summer.

Being aware of the differences discussed above between modeled and measured data in the control period, results for the A1B IPCC scenario can be analyzed. The same variations, both for wind speed and atmospheric pressure, are seen by all models, comparing the scenario and the control period. Along the coasts, all the stations show a relative increase in mean and extreme atmospheric pressure, while wind speeds tend to decrease (Table 6). The different models provide consistent information even though some perform better than others in reproducing the measured wind and atmospheric pressure statistics.

The most resolved dataset, C8E5, seems the most realistic one in describing extreme wind speed and direction changes; S18E5 reproduces better the mean value statistics, particularly for atmospheric pressure. For this specific variable, the most important aspect is the capability to propagate the information coming from the synoptic scale down to the local one, and the choice of ECHAM5 as global climate model from which to downscale seems more robust in this.

Finally, spatial models' responses to variations, analyzing the whole Adriatic Sea, can be discussed. The

E dataset does not provide substantial spatial variation in wind speed and atmospheric pressure between the control period and the A1B scenario. From Fig. 4, it is evident that the more resolved model (C8E5) simulates spatial varying changes that are also influenced by orography while in the S18E5 dataset that adopts in its setup the smoothing of Balkan orography the change is more uniform.

Focusing on the atmospheric pressure, changes are more uniformly distributed along the Adriatic Sea. This was expected because atmospheric pressure variations are large-scale features that are not so much dependent on model resolution. What is evident from Fig. 5 is that pressure increase is higher in the North Adriatic Sea than in the southern part.

5 Conclusions

This paper aimed at assessing the RCMs' capability to reproduce the meteorological climate in the Adriatic Sea for future studies of the coastal hydrodynamics. Variations in the atmospheric pressure and wind speed would change the storm surge statistics, and the combined action of the two should be assessed to define changes in the coastal hydrodynamic processes in a climate change perspective. This work allowed a first quantification of these processes observing that climate models predict an increase in atmospheric pressure of at most 0.2% that corresponds to sea level decrease of few centimeters. The major effect in the future should be connected with wind field changes. However, storminess is not only due to wind speed but also to wind direction that plays a fundamental role particularly in the North Adriatic area.

Further experiments are needed to reach definitive results, but the outcomes of this first work on the Adriatic Sea indicate the feasibility of the numerical downscaling approach from GCM to RCM ones. At the same time, they also highlight uncertainties intrinsic to this approach that may be leading, at least at the present state of the art, to results of difficult interpretation and that should be drawn with care. The numerical downscaling approach developed to study climate change impacts on coastal dynamics at the regional scale is also an innovative way to bridge the gap between the coarse information of climate scenarios from GCMs and RCMs and the detailed information necessary to investigate climate change impacts at the regional/local level. However, the different performances shown by the models considered in this study in reproducing wind and atmospheric pressure fields suggest

that the ensemble of datasets, considering the limits of each, would provide more robust climatic forcings for coastal hydrodynamic modeling implementations.

Acknowledgements The support of the European Commission through FP7.2009-1, Contract 244104—THESEUS (“Innovative technologies for safer European coasts in a changing climate”) is gratefully acknowledged. The authors want to thank the World Data Center for Climate, Hamburg, for the provision of the S18E5 dataset. Thanks also to Professor B. Rajković for producing the E dataset and Dr. E. Scoccimarro for the help in handling the E dataset. The authors also want to thank the anonymous reviewers that helped in improving this work with their precious comments.

References

- Bergamasco A, Filippetto V, Tomasin A, Carniel S (2003) Northern Adriatic general circulation behaviour induced by heat fluxes variations due to possible climatic changes. *Il Nuovo Cimento* 26(C):521–533
- Blumberg AF, Mellor GL (1986) A description of a three-dimensional coastal ocean circulation model. In: Heaps N (ed) *Three-dimensional coastal ocean models. Coastal and estuarine science*, vol 4. American Geophysical Union, Washington, DC, pp 1–16
- Djordjevic V, Rajkovic B (2008) Verification of a coupled atmosphere–ocean model using satellite observations over the Adriatic Sea. *Ann Geophys* 26:1935–1954
- Djordjevic V, Rajkovic B (2010) Development of the EBU-POM coupled regional climate model and results from climate change experiments. Nova, New York
- EU (2006) Green paper towards a future maritime policy for the union: a European vision for the oceans and seas. Presented by the commission, Brussels, COM, 275 final vol II—ANNEX
- Giorgi F, Bi X, Pal J (2004) Mean interannual variability and trends in a regional climate change experiment over Europe. *Clim Dyn* 22:733–756
- Gualdi S, Scoccimarro E, Navarra A (2008) Changes in tropical cyclone activity due to global warming: results from a high-resolution coupled general circulation model. *J Climate* 21:5204–5228
- IPCC (2007) Climate change 2007: synthesis report. Technical report, IPCC
- Jungclaus J, Keenlyside N, Botzet M, Haak H, Luo J, Marotzke J, Mikolajewicz U, Roeckner E (2006) Ocean circulation and tropical variability in the coupled model ECHAM5/MPI-OM. *J Climate* 19:3952–3972
- Kessler E (1969) On the distribution and continuity of water substance in atmospheric circulations. *Meteorol Monogr* 10:84
- Krzic A, Tosic I, Djurdjevic V, Rajkovic B (2011) Changes in some indices over serbia according to the SRES A1B and A2. *Clim Res* 49:73–86
- Orlić M, Gačić M, Violette PL (1992) The currents and circulation of the Adriatic Sea. *Oceanol Acta* 15:109–124
- Pasarić M, Orlić M (2004) Meteorological forcing of the Adriatic: present vs. projected climate conditions. *Geofizika* 21:69–87
- Pirazzoli P, Tomasin A (2003) Wind and atmospheric pressure in Venice in the 20th century: a comparative analysis

- of measurements from the meteorological stations of the Seminario Patriarcale (1901–1955) and the Istituto Cavanis (1959–2000). *Atti dell'Istituto Veneto di Scienze, Lettere ed Arti, Classe di Scienze Fisiche, Matematiche e Naturali* CLX:401–426
- Pugh D (2004) *Changing sea levels. Effect of tides, weather and climate*. Cambridge University Press, Cambridge
- Rockel B, Will A, Hense A (2008) The regional climate model COSMO-CLM (CCLM). *Meteorol Z* 17(4):347–348
- Roeckner E, Arpe K, Schlese U, Bengtsson L, Christoph M, Duemenil L, Esch M, Giorgetta M, Schulzweida U, Claussen M (1996) The atmospheric general circulation model ECHAM-4: model description and simulation of present-day climate. Max-Planck-Institut fuer Meteorologie Report
- Scoccimarro E, Gualdi S, Bellucci A, Sanna A, Fogli P, Manzini E, Vichi M, Oddo P, Navarra A (2011) Effects of tropical cyclones on ocean heat transport in a high resolution coupled general circulation model. *J Climate*. doi:10.1175/2011JCLI4104.1
- Signell RP, Carniel S, Cavaleri L, Chiggiato J, Doyle JD, Pullen J, Sclavo M (2005) Assessment of wind quality for oceanographic modelling in semi-enclosed basins. *J Mar Syst* 53:217–233
- Somot S, Sevault F, dequé M (2006) Transient climate change scenario simulation of the Mediterranean sea for the twenty-first century using a high-resolution ocean circulation model. *Clim Dyn* 27:857–879
- Somot S, Sevault F, dequé M, Crépon M (2008) 21st century climate scenario for the Mediterranean using a coupled atmosphere–ocean regional climate model. *Glob Planet Change* 63:112–126
- Tiedtke M (1989) A comprehensive mass flux scheme for cumulus parameterization in large scale models. *Mon Weather Rev* 117:1779–1800
- Tsimplis M, Marcos M, Somot S (2008) 21st century Mediterranean sea level rise: steric and atmospheric pressure contributions from a regional model. *Glob Planet Change* 63:105–111
- Vichi M, May W, Navarra A (2003) Response of a complex ecosystem model of the northern Adriatic Sea to a regional climate change scenario. *Clim Res* 24:141–158
- Woth K, Weisse R, Storch HV (2006) Climate change and North Sea storm surge extremes: an ensemble study of storm surge extremes expected in a changed climate projected by four different regional climate models. *Ocean Dyn* 56:3–15
- Zampieri M, Giorgi F, Lionello P, Nikulin G (2010) Regional climate change in the northern Adriatic. *Phys Chem Earth*. doi:10.1016/j.pce.2010.02.003